ORIGINAL ARTICLE

Turk Endod J 2025;10(2):134–141
doi: 10.14744/TEJ.2025.30922

Evaluation of fracture resistance in 3d-printed hybrid endocrowns with different preparation designs

İzim Türker Kader,[1] Safa Özer,[2] Burçin Arıcan[3]

[1]Department of Prosthodontics, Bahçeşehir University School of Dental Medicine, Istanbul, Türkiye
[2]Dental Prosthesis Technology, Bahçeşehir University Vocational School of Health Services, Istanbul, Türkiye
[3]Department of Endodontics, Bahçeşehir University School of Dental Medicine, Istanbul, Türkiye

Purpose: This in vitro study aimed to evaluate and compare the fracture resistance and failure modes of 3D-printed ceramic-filled hybrid endocrowns with four distinct preparation designs, focusing on the mechanical performance and post-endodontic restorative management.

Methods: Forty-eight 3D-printed ceramic-filled hybrid endocrowns were fabricated on 3D-printed typodont molar dies simulating endodontically treated teeth and divided into four groups (n = 12) based on preparation designs: Group A (butt joint margin, 2 mm pulp chamber depth), Group B (butt joint margin, 4 mm depth), Group C (shoulder margin, 2 mm depth), and Group D (shoulder margin, 4 mm depth). After cementation, specimens were subjected to axial loading in a universal testing machine until failure. Fracture resistance values (N) were recorded, and failure patterns were classified under 18.4x magnification. Statistical analysis was performed using a Two-Way ANOVA test ($\alpha = 0.05$).

Results: Shoulder margin designs demonstrated significantly higher fracture resistance compared to butt joint margins ($p = 0.001$), irrespective of pulp chamber depth. No significant differences were found between the 2 mm and 4 mm pulp chamber extensions ($p = 0.393$). Catastrophic (Type 4) failures were predominantly observed in Group C, while Groups A and B showed mainly repairable failure patterns.

Conclusion: Preparation design significantly affects the mechanical integrity of 3D-printed endocrowns for post-endodontic restoration. Shoulder margins enhance fracture resistance, although increasing pulp chamber depth does not confer additional mechanical benefits. These findings provide valuable insights for optimizing preparation strategies in the restorative management of endodontically treated posterior teeth.

Keywords: Dental materials; dental restoration failure; endodontically treated teeth; printing; three-dimensional.

Introduction

The common problem in restoring endodontically treated teeth is the risk of biochemical deterioration, which might be attributed to extensive loss of dental tissue that increases fracture incidence (1). Endocrowns have emerged as an innovative restoration option that preserves dental structure while enhancing mechanical durability (2). By

Cite this article as: Turker Kader I, Özer S, Arıcan B. Evaluation of fracture resistance in 3d-printed hybrid endocrowns with different preparation designs. Turk Endod J 2025;10:134-141.
Correspondence: İzim Türker Kader. Department of Prosthodontics, Bahçeşehir University School of Dental Medicine, Istanbul, Türkiye
Tel: +90 537 – 515 45 66 e-mail: izim.turker@gmail.com
Submitted: October 00, 2025 Revised: November 00, 2025 Accepted: December 00, 2025 Published: August 13, 2025

combining coronal integration with apical extension, endocrowns optimize fracture resistance and provide a reliable solution for restorative treatments (3).

The mechanical performance of endocrowns can be influenced by their preparation design, which plays a critical role in force distribution and bonding effectiveness. Common designs include a circumferential butt joint or shoulder and chamfer margins with ferrule design (4,5). A previous study utilizing lithium disilicate ceramic material has demonstrated that the shoulder margin designs increase the dentin surface available for bonding, while the butt-joint design enhances force distribution by placing the ceramic under compressive stress (6). This highlights how preparation designs can affect the mechanical performance of endocrowns by optimizing bonding and reducing the risk of fracture (7), making fracture resistance a fundamental factor in the longevity and mechanical success of endocrown restorations (8).

Material choice plays an important role in the longevity of the restoration (9). Most dental ceramics are considered brittle due to their low tensile strength and fracture toughness, which are affected by inherent flaws in the material. External loads induce tensile stresses that can trigger crack propagation from these flaws (10). To overcome the limitations of conventional all-ceramic restorations, hybrid ceramics were developed for computer-aided design and computer-aided manufacturing (CAD/CAM) by combining ceramic and composite structures, offering enhanced mechanical properties (11).

CAD/CAM systems include both subtractive and additive manufacturing, commonly known as three-dimensional (3D) printing (12). 3D printing offers several advantages over subtractive manufacturing, such as high accuracy, reduced material waste, and fabricating restorations, including undercuts or inaccessible areas that cannot be milled (13). However, only a few 3D-printed hybrid materials are available for single crowns, inlays, onlays, and veneers for anterior and posterior areas, including occlusal surfaces. Recently, VarseoSmile Triniq (Bego, Bremer, Germany), a 3D-printed ceramic-filled hybrid material, has been introduced in the market. The manufacturer claims that this material offers high dimensional stability, flexural strength and modulus, making it suitable for use as a permanent restorative material (BEGO Bremer Goldschlägerei Wilh. Herbst GmbH & Co. KG, VarseoSmile Triniq technical product information data sheet, n.d.). However, despite these claims, no studies have yet been conducted to evaluate its performance.

To the author's knowledge, while studies have evaluated the fracture resistance of CAD/CAM hybrid endocrowns fabricated via subtractive milling with various preparation designs (11,14), no research has specifically examined the fracture resistance of 3D-printed ceramic-filled hybrid endocrowns across four different preparation designs. Therefore, the aim of this in-vitro study was to compare the fracture resistance of 3D-printed hybrid endocrowns with different preparation designs. The null hypotheses tested were that (1) different preparation designs would not affect the fracture resistance of 3D-printed hybrid endocrowns, and (2) different preparation designs would not affect the failure modes of 3D-printed hybrid endocrowns.

Materials and Methods

The sample size calculation was performed using a statistical software program (G*Power v3.1.9.2, Heinrich Heine University, Düsseldorf, Germany) using data from another study by Einhorn et al (6). The minimum sample size of 12 specimens for each group achieved 95% power to detect differences, with a significance level of 0.05, to test the null hypotheses.

Teeth Preparation

Typodont maxillary first molar teeth (AG-3 ZE; Frasaco GmbH, Tettnang, Germany) were prepared according to four preparation designs by one operator (S.Ö). The preparations were performed under a dental microscope (Zumax OMS 2000, Zumax, China) at x18.4 magnification. The preparation groups were as follows:

- Group A: Butt-joint margin and a 2 mm pulp chamber depth
- Group B: Butt-joint margin and a 4 mm pulp chamber depth
- Group C: Shoulder (1 mm) margin and a 2 mm pulp chamber depth
- Group D: Shoulder (1 mm) margin and a 4 mm pulp chamber depth

The following burs were used for the preparation of Group A and B, respectively:

- A green belt occlusal-reduction diamond bur (D.828.017.G.FGA; Frank Dental GmbH, Gmund, Germany) for 2 mm occlusal reduction
- A green belt wheel diamond bur (909G-031-FG Coarse 5/Pk; Meisinger, Neuss, Germany) for 2 mm wide circumferential butt-joint margin preparation
- A red belt conical diamond bur (D.845KR.016.G.FGA; Frank Dental GmbH, Gmund, Germany) for pulp chamber preparation with an internal taper of 8° axial walls (15).
- A red belt medium round-end tapered diamond bur (D.850.016.FG; Frank Dental GmbH, Gmund, Germany) to round down internal lines, eliminate irregularities, and

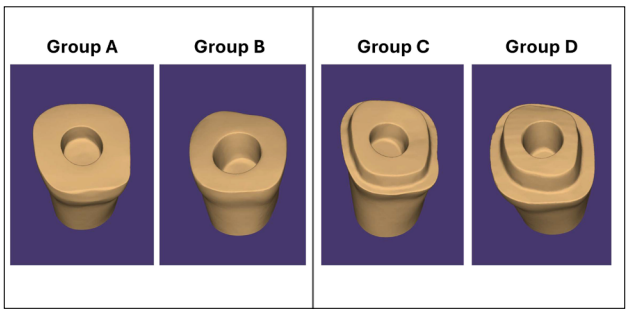

Fig. 1. Preparation scan images obtained using a digital intraoral scanner for Group A, Group B, Group C, and Group D.

create flat and polished surfaces.

For Groups C and D, identical burs were used throughout the whole preparation process in Groups A and B. The primary difference in contrast to Groups A and B was the following bur:

• A red belt modified shoulder fine W diamond bur (848WF-018-FG; Meisinger, Gmund, Germany) to prepare the 1 mm shoulder margin following the first occlusal reduction step.

The preparation designs of all groups are shown in Fig. 1. Following the preparations, a digital calliper (Micrometer; Mitutoyo Corp., Tokyo, Japan) and a periodontal probe were used to confirm the measurements of pulp chamber depths, margin widths, and occlusal reductions.

Master die fabrication

The prepared teeth for each group were scanned using a digital intraoral scanner CEREC AC Primescan (Dentsply Sirona, York, PA, USA). The external CAD data of preparation scans were processed in InEos X5 software (Dentsply Sirona, York, PA) (Fig. 1). Standard tessellation language (STL) files were obtained and imported by a CAD program (Sharp 3D, Budapest, Hungary) for generating and creating ready models. A total of 48 single master dies with a layer thickness of 50 µm were fabricated from 3D-printed model resin (VarseoWax Model; Bego, Bremer, Germany) using a 3D printer (Asiga Ultra (50), Sydney, Australia). After printing, the master dies were rinsed with 99 % isopropanol alcohol for 3 minutes (Form Wash, Formlabs®, Somerville, USA) and post-cured twice for 20 minutes at 60 °C (Form Cure, Formlabs®, Somerville, USA) following the manufacturer's instructions.

Endocrown design

The typodont maxillary molar teeth were scanned before and after each preparation, and STL data were obtained from each scan. The preparation STL files were used for endocrown design, while the initial STL data represented the original tooth morphology. All STL data were processed using exocad DentalCAD software (exocad GmbH, Darmstadt, Germany). The cement space was specified at 80 µm in the chairside CAD design. The endocrowns were fabricated with a 50 µm layer thickness from 3D-printed ceramic-filled hybrid material, VarseoSmile Triniq, using the 3D printer. The printed endocrowns were cleaned with 99% isopropanol alcohol for 5 minutes and post-cured twice for 20 minutes at 60 °C.

Endocrown Cementation

Endocrowns were loaded with self-adhesive dual-cure resin cement (Dentacore; ITENA Clinical, Paris, France) and seated on their corresponding teeth. While seating, a standardized constant load was applied using a weight of 50 N to prevent the restoration's rebounding during cementation. Any residual cement was cleaned with a micro brush (TPC Advanced Technology Inc., CA, USA). Then, endocrowns were light-cured for 20 seconds from all surfaces to ensure complete polymerization of the resin cement (16). After setting, residual cement was gently removed from the margins using a no.12 surgical blade (Feather Safety Razor Co. Ltd., Osaka, Japan) under the dental microscope.

Fracture resistance test

Before subjecting to the fracture resistance test, the roots of the specimen were shielded by a 0.2 mm C-silicone putty impression material (Zetaplus, Zhermack, Italy) for the periodontal ligament simulation. Vaseline was applied inside plastic moulds with a height of 3 cm to provide insulation. Auto-polymerizing acrylic resin (Imicryl Dental, Konya, Turkey) were mixed according to the manufacturer's recommendations and poured inside the moulds. Then, the specimens were inserted into acrylic resin up to 2 mm below the cementoenamel junction (CEJ) level of master dies (17). The CEJ was determined and marked 10 mm below the occlusal surface, considering that the crown height of the maxillary first molar teeth was approximately 8 mm. After the polymerization was completed, the acrylics were removed from the plastic moulds. The occlusal surface distance of the endocrowns was measured with the digital calliper, and a mark was placed at the center point corresponding to the central fossa. The acrylics in which the specimens were embedded were fixed to a custom-designed metal plate produced in accordance with the universal testing machine (MIN 100; Esetron, Ankara, Turkey) and a fracture test was performed. Each sample was loaded using a metallic loading rod with a spherical tip (3.4 mm diameter) travelling at a crosshead speed of 1 mm/min. The loading rod was adjusted to exactly match the marked point, and the load was applied along the long

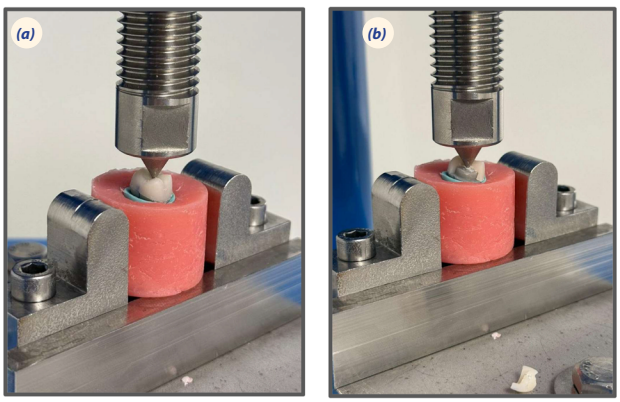

Fig. 2. **(a)** Placement of the acrylic block with the embedded endocrown into the universal testing machine and application of axial loading until the maximum fracture load is reached **(b)** Representative image of a fractured endocrown specimen.

axis of the specimens (Fig. 2A). The maximum axial load until the fracture occurred was applied over specimens (Fig. 2B). The fracture load was measured in Newton (N) and recorded using the corresponding software of the testing machine.

Failure mode evaluation

Following the fracture resistance test, the failure modes of all specimens were evaluated using the dental operation microscope at magnification x18.4. Specimens were categorized according to fracture pattern examination as follows (18):

- Type 1: Complete or partial debonding of the endocrown without fracture (favorable failure) (Fig. 3A)
- Type 2: Fracture of the endocrown without tooth fracture (favorable failure) (Fig. 3B)
- Type 3: Fracture of the endocrowns or tooth above the level of CEJ (favorable failure) (Fig. 3C)
- Type 4: Fracture of the endocrowns or tooth below the level of CEJ (non-favorable or catastrophic failure) (Fig. 3D)
- Examples of two failure types occurring together were observed in each group (Fig. 3E; Fig. 3F).

Statistical Analysis

The data were analyzed using Minitab V14 (Minitab Inc., State College, PA, USA). The normality of distribution was assessed with the Shapiro-Wilk Test. A Two-Way ANOVA was used to compare the parameters that were normally distributed according to margin design and pulp chamber depth. Descriptive statistics for fracture resistance were presented as mean ± standard deviation. The significance level was set as $p < 0.05$.

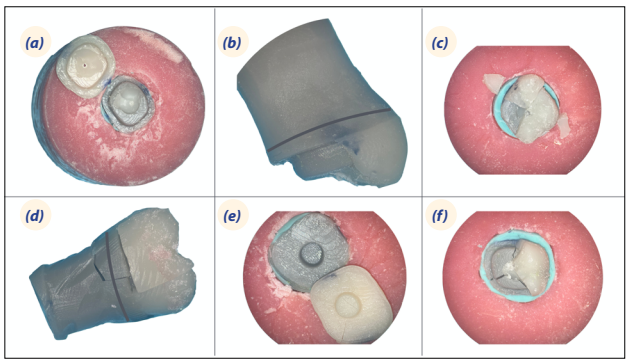

Fig. 3. The figure shows different failure modes of endocrown specimens **(a)** Type 1 **(b)** Type 2 **(c)** Type 3 **(d)** Type 4 **(e)** The combination of Type 1 and Type 2 **(f)** The combination of Type 2 and Type 3 failure modes. *Black lines indicate the cementoenamel junction (CEJ).

Results

The effects of margin design and pulp chamber depth on fracture resistance of 3D-printed hybrid endocrowns and the interaction between the two are shown in Table 1. Margin design was found to have a statistically significant main effect on fracture resistance ($p < 0.05$), whereas pulp chamber depth alone did not show statistical significance ($p > 0.05$). Furthermore, the interaction between margin design and pulp chamber depth was not statistically significant ($p > 0.05$) (Table 1).

Descriptive statistics and multiple comparisons of fracture resistance values according to margin design and pulp chamber depth are shown in Table 2 and Fig. 4. The shoulder margin design showed a significantly higher mean value of 660.12 ± 171.63 N, whereas the mean fracture resistance for the butt joint design was 503.44 ± 134.81 N ($p < 0.05$). The results demonstrated that the margin design consistently influenced fracture resistance across both pulp chamber depths. Although the highest fracture resistance of 678.52 ± 207.52 N was observed for the shoulder design and a 2 mm pulp chamber depth (Group C), this difference was not statistically significant (Table 2) (Fig. 4).

Failure modes are shown in Table 3. Regarding failure

Table 1. Comparison of fracture resistance values according to margin design and pulp chamber depth

	F	p	η^2
Margin design	12.034	0.001	0.215
Pulp chamber depth	0.744	0.393	0.017
Margin design*Pulp chamber depth	0.002	0.962	0.000

F: Two-Way ANOVA Test Statistic; η2: Partial Eta Square. Statistically significant at $p < 0.05$.

Table 2. Multiple comparisons of the mean fracture resistance values according to margin design and pulp chamber depth

Margin design	Pulp chamber depth		Mean ± SD
	2 mm	4 mm	
Shoulder	678.52 ± 207.52A	641.73 ± 133.38A	660.12 ± 171.63
Butt joint	524 ± 176.82B	482.87 ± 76.21B	503.44 ± 134.81
Mean ± SD	601.26 ± 204.4	562.3 ± 133.68	581.78 ± 171.98

Mean ± Standard Deviation (SD); No difference between values with the same letter. Statistically significant at $p < 0.05$.

Table 3. Numbers of different failure modes for endocrown groups with different preparation designs

	Type 1	Type 2	Type 3	Type 4
Group A	1	9	9	1
Group B	1	11	11	0
Group C	1	4	8	3
Group D	1	8	9	1

Examples of two failure types occurring together were observed in each group.

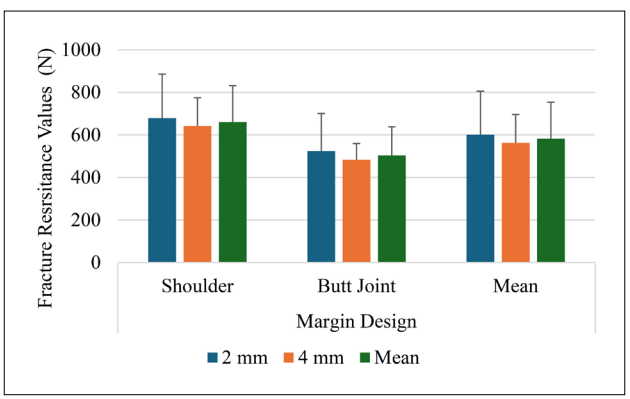

Fig. 4. The column chart of fracture resistance values of endocrowns with different preparation designs.

modes, no differences were observed among the groups for type 1 failure. However, type 2 and type 3 failures were most frequent in Group B, followed by Group A and Group D. Group B also exhibited the lowest incidence of type 4 failure, whereas Group C showed the highest incidence of type 4 failure. Examples of two failure types occurring together were observed in each group (Fig. 3E; Fig. 3F).

Discussion

The long-term success of dental restorations depends significantly on their ability to resist fractures and withstand the functional forces encountered during mastication. Endocrowns have emerged as a reliable post-endodontic restorative option for posterior endodontically treated teeth, offering both esthetic and mechanical benefits (19). In this study, the fracture resistance and failure modes of endocrown restorations fabricated using a 3D-printed ceramic-filled hybrid material were evaluated against different preparation designs. The results demonstrated that both null hypotheses were rejected, indicating that preparation design significantly affected both fracture resistance and failure modes of endocrown restorations.

The mechanical performance of endocrowns can be significantly influenced by variations in preparation, including margin design and preparation depth (4,5). Forces acting on endocrown are distributed as compressive forces over the cervical butt joint margin or as shear forces along the axial walls of the shoulder margin design (3). Taha et al. (4) reported that adding a short axial wall and shoulder finish line (ferrule design) into the preparation of endodontically treated teeth restored with endocrowns enhances higher fracture resistance compared to the butt joint margin design. This may result from the ability of the axial walls of shoulder margin design to counteract shear stresses and facilitate better load distribution along the margin, thereby increasing the fracture resistance (3). Similarly, a study by Hassan et al. (20) demonstrated that endocrowns with a ferrule design showed higher fracture resistance than those without. Consistent with the findings of these studies, the current study revealed that a circumferential shoulder margin design showed a greater mean fracture resistance compared to the butt joint margin. In contrast, Al-khafaji and Jasim (21) found that endocrowns with butt joint preparation in maxillary first premolars showed higher fracture resistance than those with a ferrule design. This discrepancy may be attributed to differences in teeth group and restoration type and material, as they utilized natural premolar teeth and lithium disilicate endocrowns in their study, whereas the present study used 3D-printed ceramic-filled hybrid materials over 3D-printed molar dies. Notably, the use of restorative materials with comparable microstructures may have resulted in similar fracture resistance outcomes against different margin designs (4).

The influence of preparation depth on fracture resistance

of endocrowns has been the subject of ongoing discussion, with evidence suggesting that deeper pulp chamber preparation may enhance their mechanical performance by increasing load to failure and reducing stress concentration (5). Dartora et al. (22) reported that a 5 mm pulp chamber depth presented a higher load to failure than a 1 mm depth, while Hayes et al. (23) found that a 4 mm depth exhibited greater fracture resistance compared to 2 mm, both using lithium disilicate ceramics. Conversely, De Kuijper et al. (24) and Ghajghouj et al. (25) reported no significant correlation between pulp chamber depth and fracture resistance. In agreement with the latter studies, the present study found no statistically significant difference between 2 mm and 4 mm pulp chamber depths. This variation may be explained using different materials across studies, as the material used in this study differs in composition compared to the lithium disilicate ceramics mentioned in previous studies.

The evaluation of failure modes is a crucial factor in understanding the long-term mechanical performance of restorations (26). In this study, fracture patterns were categorized into four types. Type 4 was defined as nonfavorable or catastrophic failure, where the fracture of the endocrown occures below the CEJ. Previous studies have classified failures as favorable or repairable when the fracture is at or coronal to the CEJ and irreparable when the fracture is apical to the CEJ (27). Accordingly, in this study, Type 1, Type 2, and Type 3 failure modes were considered repairable, while Type 4 was deemed irreparable. The failure mode evaluation revealed that Group C presented the highest incidence of Type 4 catastrophic failure, while Group A and B predominantly exhibited Type 2 and Type 3 favorable failures (Table 3). These findings aligned with Einhorn et al. (6), who reported in their study that higher catastrophic failures were associated with a 2 mm ferrule design. Similarly, Magdy et al. (14) found that endocrowns with butt joint margin design exhibited a higher percentage of repairable failures. Al-shibri and Elguindy (16) supported this by reporting that endocrowns with butt joint margin design fabricated from hybrid nanoceramics showed 70% of repairable fractures compared to 30% of irreparable fractures apical to the CEJ. In the present study, the butt joint margin design showed both lower fracture resistance and favorable failure modes. This may be attributed to the stable surface provided by the butt joint design, which resists compressive stresses due to its preparation parallel to the occlusal plane. Additionally, from a biomechanical perspective, this design allows strain adaptation at the interface between the tooth and restoration. However, Magne et al. (28) suggested that the axial reduction in the shoulder finish line could reduce resin cement thickness relative to the bulk of the material, thereby decreasing stress on the material. Considering that the shoulder margin design in this study showed higher fracture resistance values, further studies are necessary to evaluate stress concentrations of endocrown restorations with different preparation designs.

The incidence of catastrophic failure was lower across all groups than other types of failures. This can likely be attributed to the superior shock-absorbing capacity of hybrid ceramic materials compared to all ceramic materials (29). The microstructure of hybrid ceramics may enhance their resistance to crack propagation, which contributes to their lower incidence of catastrophic failures. Supporting this, a previous study has shown that lithium disilicate ceramic endocrowns presented a higher percentage of catastrophic failures compared to hybrid ceramics (30). This difference may be due to the rigidity of materials like lithium disilicate, which can exhibit stress concentrations in critical areas and cause severe fractures, whereas materials with a lower elastic modulus can better distribute stress under load (31).

The maximum chewing force was reported as approximately 850 N, considered a normal force in the molar region (22). This means that the mean fracture resistance for all groups was below the maximum chewing forces reported in the literature. However, considering that this force will be distributed to the premolar and molar teeth in the chewing area, the mean fracture resistance value of all groups, 581.78 ± 171.98 N, may be acceptable.

To strengthen the validity of this study, standardized typodont teeth and 3D-printed master dies were used, which made it possible to precisely control preparation design variables and minimize the variability typically seen between extracted natural teeth, such as differences in size, morphology, or bonding quality caused by variations in enamel and dentin. In addition, using resin models helps overcome common challenges associated with biological specimens, such as the need for ethical approval, the risk of cross-infection, and complex storage requirements, ultimately making laboratory workflows both safer and more streamlined (32). To further ensure reproducibility, all preparations were performed by a single operator after multiple trials. Importantly, a cement space of 80 µm was set in the CAD software, as this intermediate value aligns with the optimal settings reported for both ceramic materials (60 µm) and resin composites (120 µm) (33), reflecting the hybrid microstructure of the 3D-printed material used. The endocrowns were cemented onto the dies using self-adhesive resin cement. As natural human teeth were not used in this study, a one-step cementation procedure was performed without the need for pretreatment, such as

etching, primer, or bonding agent application. Periodontal ligament simulation was also incorporated by applying a thin layer of silicone impression material over the root portion of the dies to better mimic clinical stress conditions (34).

This in vitro study has several limitations. First, the evaluation of stress distribution within the material was not conducted using finite element analysis, which may provide insights into the failure modes of restoration. Additionally, the force applied experimentally had only an axial vector, omitting lateral or oblique forces that may arise from parafunctional movements and affect clinical performance. Furthermore, the use of 3D-printed resin models, while offering the advantage of experimental standardization, does not fully replicate the mechanical and histological properties of natural dentin. Interestingly, Munoz-Sanchez et al. (35) reported that although 3D-printed model resin cannot entirely replace natural teeth in resistance testing, they show lower variance in mean strength values, allowing better control over natural variability in tooth size and shape. This highlights that while 3D-printed models offer a useful platform for initial biomechanical evaluations, future studies should complement these findings by incorporating natural teeth to strengthen the clinical relevance and applicability of the results. Additionally, integrating advanced methodologies such as finite element analysis and in vivo studies could further enhance our understanding of the performance of different preparation designs and materials under complex loading conditions.

Conclusion

Based on the findings of this study, margin design significantly influenced the fracture resistance and failure modes of 3D-printed ceramic-filled hybrid endocrowns. Shoulder margins exhibited superior fracture resistance over butt-joint designs, while pulp chamber depth alone did not yield significant benefits. Notably, a 2 mm pulp chamber depth with a shoulder margin showed a higher incidence of catastrophic failure compared to a 4 mm depth, suggesting the interplay of preparation geometry and material properties. Overall, the combination of a 1 mm shoulder margin with a 4 mm pulp chamber depth enhanced fracture resistance and promoted favorable failure modes.

Authorship Contributions: Concept: İ.T.K., S.Ö., B.A.; Design: İ.T.K., S.A.; Supervision: B.A..; Fundings: İ.T.K., S.Ö., B.A.; Data Collection and/ or Processing: İ.T.K., S.Ö.; Analysis and/ or Interpretation: İ.T.K., B.A.; Literature Review: İ.T.K., B.A.; Writer: İ.T.K.; Critical Review: B.A.

Use of AI for Writing Assistance: Not declared

Source of Funding: None declared.

Conflict of Interest: None declared.

Ethical Approval: Not applicable.

Informed consent: Not applicable.

References

1. Schwartz RS, Robbins JW. Post placement and restoration of endodontically treated teeth: A literature review. J Endod 2004; 30(5): 289–301. [CrossRef]
2. Al-Dabbagh RA. Survival and success of endocrowns: A systematic review and meta-analysis. J Prosthet Dent 2021; 125(3): 415.e1–9. [CrossRef]
3. Fages M, Bennasar B. The endocrown: A different type of all-ceramic reconstruction for molars. J Can Dent Assoc 2013; 79: d140.
4. Taha D, Spintzyk S, Schille C, et al. Fracture resistance and failure modes of polymer infiltrated ceramic endocrown restorations with variations in margin design and occlusal thickness. J Prosthodont Res 2018; 62(3): 293–7. [CrossRef]
5. Kanat-Ertürk B, Saridağ S, Köseler E, et al. Fracture strengths of endocrown restorations fabricated with different preparation depths and CAD/CAM materials. Dent Mater J 2018; 37(2): 256–65. [CrossRef]
6. Einhorn M, DuVall N, Wajdowicz M, et al. Preparation ferrule design effect on endocrown failure resistance. J Prosthodont 2019; 28(1): e237–42. [CrossRef]
7. Akbar JH, Petrie CS, Walker MP, et al. Marginal adaptation of Cerec 3 CAD/CAM composite crowns using two different finish line preparation designs. J Prosthodont 2006; 15(3): 155–63. [CrossRef]
8. Contrepois M, Soenen A, Bartala M, et al. Marginal adaptation of ceramic crowns: A systematic review. J Prosthet Dent 2013; 110(6): 447–54.e10. [CrossRef]
9. Ghoul WE, Ozcan M, Silwadi M, et al. Fracture resistance and failure modes of endocrowns manufactured with different CAD/CAM materials under axial and lateral loading. J Esthet Restor Dent 2019; 31(4): 378–87. [CrossRef]
10. Sterzenbach G, Karajouli G, Tunjan R, et al. Damage of lithium-disilicate all-ceramic restorations by an experimental self-adhesive resin cement used as core build-ups. Clin Oral Investig 2015; 19(2): 281–8. [CrossRef]
11. Zimmermann M, Ender A, Egli G, et al. Fracture load of CAD/CAM-fabricated and 3D-printed composite crowns as a function of material thickness. Clin Oral Investig 2019; 23(6): 2777–84. [CrossRef]
12. Sidhom M, Zaghloul H, Mosleh IES, et al. Effect of different CAD/CAM milling and 3D printing digital fabrication techniques on the accuracy of PMMA working models and vertical marginal fit of PMMA provisional dental prosthesis: An in vitro study. Polymers (Basel) 2022; 14: 1285. [CrossRef]

13. Ahlholm P, Lappalainen R, Lappalainen J, et al. Challenges of the direct filling technique, adoption of CAD/CAM techniques, and attitudes toward 3D printing for restorative treatments among Finnish dentists. Int J Prosthodont 2019; 32: 402–10. [CrossRef]
14. Magdy H, Mahallawi O, Nabil O. Efficacy of preparation design on fracture resistance of hybrid-ceramic endocrown on premolars: An in vitro study. Int J Appl Dent Sci 2023; 9(1): 12–8. [CrossRef]
15. Sun J, Ruan W, He J, et al. Clinical efficacy of different marginal forms of endocrowns: Study protocol for a randomized controlled trial. Trials 2019; 20(1): 454. [CrossRef]
16. Al-shibri S, Elguindy J. Fracture resistance of endodontically treated teeth restored with lithium disilicate crowns retained with fiber posts compared to lithium disilicate and cerasmart endocrowns: In vitro study. Dentistry 2017; 7(12): 464. [CrossRef]
17. Marchionatti AM, Wandscher VF, Broch J, et al. Influence of periodontal ligament simulation on bond strength and fracture resistance of roots restored with fiber posts. J Appl Oral Sci 2014; 22(5): 450–8. [CrossRef]
18. El-Damanhoury HM, Haj-Ali RN, Platt JA. Fracture resistance and microleakage of endocrowns utilizing three CAD-CAM blocks. Oper Dent 2015; 40(2): 201–10. [CrossRef]
19. Bindl A, Mörmann WH. Clinical evaluation of adhesively placed Cerec endo-crowns after 2 years--preliminary results. J Adhes Dent 1999; 1(3): 255–65.
20. Hassan SM. Effect of different preparation designs on the fracture resistance of IPS E.max CAD Endo-Crowns. ASDJ 2020; 19(3): 40–9. [CrossRef]
21. Al-khafaji S, Jasim H. Fracture resistance of endodontically treated teeth restored by full crown and two endocrowns preparation design made from lithium disilicate material. Int J Med 2020; 25: 31–42.
22. Dartora NR, de Conto Ferreira MB, Moris ICM, et al. Effect of intracoronal depth of teeth restored with endocrowns on fracture resistance: In vitro and 3-dimensional finite element analysis. J Endod 2018; 44(7): 1179–85. [CrossRef]
23. Hayes A, Duvall N, Wajdowicz M, et al. Effect of endocrown pulp chamber extension depth on molar fracture resistance. Oper Dent 2017; 42(3): 327–34. [CrossRef]
24. de Kuijper M, Cune MS, Tromp Y, et al. Cyclic loading and load to failure of lithium disilicate endocrowns: Influence of the restoration extension in the pulp chamber and the enamel outline. J Mech Behav Biomed Mater 2020; 105: 103670. [CrossRef]
25. Ghajghouj O, Tasar-Faruk S. Evaluation of fracture resistance and microleakage of endocrowns with different intracoronal depths and restorative materials luted with various resin cements. Materials (Basel) 2019; 12(16): 2528. [CrossRef]
26. Mostafavi AS, Allahyari S, Niakan S, et al. Effect of preparation design on marginal integrity and fracture resistance of endocrowns: A systematic review. Front Dent 2022; 19: 37. [CrossRef]
27. Abdel-Aziz MS, Abo-Elmagd AA. Effect of endocrowns and glass fiber post-retained crowns on the fracture resistance of endodontically treated premolars. Egypt Dent J 2015; 61(3): 3203–10.
28. Magne P, Versluis A, Douglas WH. Effect of luting composite shrinkage and thermal loads on the stress distribution in porcelain laminate veneers. J Prosthet Dent 1999; 81(3): 335–44. [CrossRef]
29. Leung BT, Tsoi JK, Matinlinna JP, et al. Comparison of me¬chanical properties of three machinable ceramics with an experimental fluorophlogopite glass ceramic. J Prosthet Dent 2015; 114(3): 440–6. [CrossRef]
30. Argyrou R, Thompson GA, Cho SH, et al. Edge chipping resis¬tance and flexural strength of polymer infiltrated ceramic network and resin nanoceramic restorative materials. J Prosthet Dent 2016; 116(3): 397–403. [CrossRef]
31. Yara A, Goto SI, Ogura H. Correlation between accuracy of crowns fabricated using CAD/CAM and elastic defor¬mation of CAD/CAM materials. Dent Mater J 2004; 23(4): 572–6. [CrossRef]
32. Reis T, Barbosa C, Franco M, et al. 3D-printed teeth in endodontics: Why, how, problems and future—A narrative review. Int J Environ Res Public Health 2022; 19(13): 7966. [CrossRef]
33. Zheng Z, Wang H, Mo J, et al. Effect of virtual cement space and restorative materials on the adaptation of CAD-CAM endocrowns. BMC Oral Health 2022; 22(1): 580. [CrossRef]
34. Soares CS, Pizi ECG, Fonseca RB, et al. Influence of root embedment material and periodontal ligament simulation on fracture resistance tests. Braz Oral Res 2005; 19(1): 11–6. [CrossRef]
35. Munoz-Sanchez ML, Gravier A, Francois O, et al. In vitro resistance of natural molars vs. additive-manufactured simulators treated with pulpotomy and endocrown. J Funct Biomater 2023; 14(9): 444. [CrossRef]